Permeability, Diffusivity, and Solubility of Oxygen Gas in Liquid Slag

M. SASABE AND K. S. GOTO

An experimental procedure for measurement of the permeability of dissolved oxygen gas in liquid slag has been developed using an oxygen concentration cell. The small amount of oxygen gas which penetrated through the liquid oxide from a pure oxygen compartment to a pure argon compartment was determined by the galvanic cell. The permeabilities of oxygen through liquid $PbO-SiO_2$ and $FeO-PbO-SiO_2$ were found to be in the range 3×10^{-8} to 3×10^{-7} moles/cm·s. The permeabilities were little influenced by temperature but more influenced by the composition. In separate experiments, the oxygen pressure change at the bottom of a column of slag was detected by another galvanic cell. By this method, it is not necessary to quench the specimen to determine the concentration profile of dissolved oxygen and to determine its diffusivity. Liquid oxides in the $PbO-SiO_2$, $CaO-SiO_2-Al_2O_3$ and $FeO-PbO-SiO_2$ systems were studied. The oxygen diffusion coefficients (5×10^{-5} to 3×10^{-3} cm^2/s) were found to increase with temperature for a fixed composition of slag, and with an increase of network-modifier oxide content at constant temperature. The solubility of oxygen gas in $PbO-SiO_2$ melts was estimated to be 2×10^{-4} to 2×10^{-5} moles/cm^3 from the determined diffusivities and permeabilities. The solubilities decreased with increasing temperature in the composition range studied. Physical solubilities of gases and metals in slags determined by other investigators are compared with the present results.

In 1959, Greene and his co-workers published two papers,[1,2] in which they measured the rate of absorption of pure oxygen gas bubbled into liquid alkali alumina silicate glass. These studies are among the very few direct measurements of oxygen gas absorption into liquid oxide mixtures containing no transition metals. However, only the product of the oxygen diffusivity and solubility was approximately obtained.

In the present work, the permeability and diffusivity of oxygen gas through oxide melts have been independently measured, and from these two quantities the solubility is estimated.

Oxygen gas can be physically dissolved in liquid oxides as diatomic molecules[3] according to the reaction

$$O_2\ (\text{gas phase}) \rightarrow O_2\ (\text{dissolved in oxide melt}) \qquad [1]$$

When the melt contains a transition metal oxide, the oxygen gas can be chemically dissolved according to the reaction

$$2M^{2+}\ (\text{in melt}) + \tfrac{1}{2}O_2\ (\text{gas}) \rightarrow 2M^{3+}\ (\text{in melt}) + O^{2-}\ (\text{in melt}) \qquad [2]$$

where M^{2+}, M^{3+}, and O^{2-} are divalent and trivalent metal cations, and divalent oxygen anions in the melt. Oxygen that dissolves in this way enters merely the anionic lattice of O^{2-} ions, and is not different from the O^{2-} that is already contributed by the ionization of metal oxides. Thus, all metal oxide melts contain relatively large concentrations of oxygen anions relative to physically dissolved diatomic oxygen gas. However, the oxygen anions do not contribute to the transport of oxygen through the oxide melt as long as there is no electronic conductivity in the melt.

M. SASABE is Research Associate, Tokyo Institute of Technology, presently at Technische Hochschule Aachen, West Germany. K. S. GOTO is Associate Professor, Tokyo Institute of Technology, Megro-ku, Ookayama, Tokyo, Japan.

Manuscript submitted September 25, 1973.

The present work was carried out mainly with liquid mixtures of network modifiers, *e.g.*, PbO, Na_2O, CaO, and network formers, *e.g.*, SiO_2, Al_2O_3, GeO_2, which contained no transition metal oxides. Thus, physical dissolution of oxygen seems more likely to be predominant than chemical dissolution. The latter was studied in a few experiments by adding iron oxide.

An oxygen concentration cell has been used to determine the very small quantity of oxygen gas which permeated through liquid oxide mixtures from a pure oxygen gas compartment to a pure argon gas compartment.

For the diffusivity determination, the previous electrochemical method[4,5] to detect the oxygen pressure change in the oxide melt has been modified to enable the calculation of diffusivity. Because the present work deals mainly with the physical dissolution of oxygen gas and its transport in liquid oxides containing no transition metals, the results can be discussed in comparison to the physical solubilities of several other elements in liquid oxides.

The physical solubility and diffusivity of helium gas and neon gas in oxide melts have been determined by Mulfinger and Scholze[6] and by Frischat and Oel.[7] The physical and chemical solubility of nitrogen gas was studied by Mulfinger and Meyer,[8] and by Mulfinger,[9] while the physical solubility of metals in silicate melts was measured for copper and silver by Richardson and Billington[10] and for gold and lead by Meyer and Richardson.[11] From these studies, one may draw the following conclusions for the physical solubility of elements in oxide melts:

1) The solubility is proportional to the partial pressure of the element in the gas phase for a fixed oxide composition and temperature.

2) The solubility increases with increasing temperature at a fixed oxide composition, and with an increase of the content of network-forming oxides at a constant temperature.

3) For a fixed oxide composition and temperature,

the solubility of the elements decreases with an increase in the atomic or molecular radius of the dissolved elements.

4) The above results suggest that the neutral atoms and molecules fit into the electrically-neutral holes in the silicate or aluminate networks.

For the diffusion coefficients of helium and neon, the following are the results of the studies by Mulfinger and Scholze[6] and by Frischat and Oel.[7]

1) The diffusion coefficient increases with temperature for a fixed oxide composition.

2) The diffusion coefficient decreases with an increase in the content of acidic oxide at a constant temperature.

3) The mechanism of diffusion is interpreted by the combination of the movement of spherical atoms through a viscous liquid and the movement through channels or holes in the network structure in the oxide melts.

I. EXPERIMENTAL PROCEDURE

1-1. Measurement of Permeability

The experimental apparatus is shown in Fig. 1. The gas phase in the reaction chamber is separated into two compartments separated by the liquid slag in the crucible. To one of them pure oxygen gas is admitted and to the other purified argon gas. Thus, oxygen gas will penetrate through the liquid slag from the pure oxygen compartment to the argon compartment. The permeability through the solid alumina tube was measured and shown to be negligibly small.

The flow rate of purified argon gas was fixed at a constant value of 1500 (STP) cc/min and the steady state oxygen content of the outlet gas was determined by an oxygen concentration cell in a separate furnace. The partial pressure of oxygen in the purified argon was 10^{-8} atm, although this increased to 5×10^{-8} atm upon performing a blank run. As the range of oxygen pressures in the outlet gas for actual measurements was 10^{-5} to 10^{-4} atm, the oxygen content of the blank could be neglected.

Liquid slag was melted in a fused alumina crucible (99.8 wt pct Al_2O_3), then a fused alumina tube (99.8 wt pct Al_2O_3) shown as the shield tube in Fig. 1 was dipped in the molten slag. The depth of the liquid slag was about 2.0 cm and the shield was immersed to about 1.0 cm. The inner and outer diameters of the alumina crucible were 2.0 and 2.5 cm, and of the shield tube, 0.6 and 1.0 cm. The crucible assembly was set in the reaction chamber. The outlet gas with a steady state oxygen content was led to a separate furnace, in which an oxygen concentration cell was heated to 900°C was used to determine the oxygen content. The oxygen concentration cell, with a solid electrolyte of stabilized zirconia, had as its reference electrode a mixture of metallic nickel and nickel oxide powder. Platinum wires were used as the electrodes. A chromel-alumel thermocouple on the surface of the solid electrolyte was used for temperature measurement. The oxygen concentration cell was calibrated against air before each experimental run.

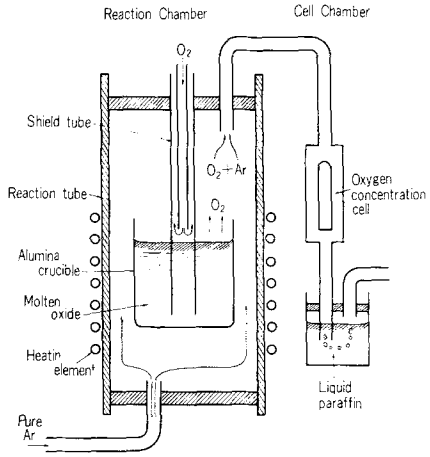

Fig. 1—Schematic diagram of experimental apparatus used for permeability measurements.

The permeability is defined by

$$\mathbb{P} \equiv J \cdot \frac{l}{A} \qquad [3]$$

where $\mathbb{P}$ is the permeability expressed in moles O_2 gas/cm · s, J is the rate of oxygen gas transfer through the liquid slag when pure oxygen gas is in the one compartment and pure argon in the other and is expressed in moles O_2 gas/s, l is the effective length of the diffusion path in cm, and A is the effective cross-section of the diffusion path in cm^2.

In the present method, A and l cannot be measured directly. However, the ratio of A to l, called the cell constant, can be determined from measurement of the permeability of oxygen gas through liquid silver under the same conditions, since the oxygen diffusivity is well established.[12,13,14,15,16,17] The permeability of oxygen gas through liquid silver can be expressed by

$$\mathbb{P} = J \cdot \frac{l}{A} = J \cdot K = D_0(C^0 - C_{\text{argon}}) \qquad [4]$$

where D_0 is the diffusion coefficient of oxygen in liquid Ag, C^0 is the solubility of oxygen gas in liquid Ag under pure oxygen gas at 1 atm in gram-atoms $\underline{O}/cm^3$, and C_{argon} is the solubility of oxygen gas in liquid Ag in the argon compartment, which can be approximately taken as zero. K is the cell constant in cm^{-1} and can be determined from the measured oxygen transfer rate, J, and values of D_0 and C^0 (under pure oxygen gas) given in the literature. Sieverts and Hagenacker[18] express the solubility of oxygen as follows:

$$\log_{10}[\text{wt pct O}] = \frac{737.6}{T} - 1.107 \qquad [5]$$

The density of silver is 9.20 g/cm^3 (Ref. 19) at 1000°C,

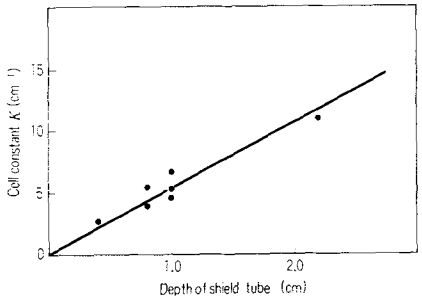

Fig. 2—Relation between the depth of the shield tube (see Fig. 1) and cell constant when the diameters of the crucible and the shield tube are held constant.

so that C^0 becomes 1.70×10^{-3} g-atm O/cm^3 at 1000°C. Velho *et al*[15] give the following equation for the diffusivity of oxygen:

$$D_0 = 2.2 \times 10^{-3} \exp\left[\frac{-7900}{RT}\right] \qquad [6]$$

These data are selected simply because these results are almost equal to the mean values of different investigators and are among the oldest. Fig. 2 shows how the experimental cell constant changes with the depth of immersion of the shield tube (see Fig. 1) for constant diameters of crucible and shield.

1-2. Measurement of Diffusivity

The experimental apparatus is shown in Fig. 3. The side-wall of the lime stabilized zirconia electrolyte tube was insulated from the slag by a fused alumina tube. Only the outside-bottom of the electrolyte tube contacted both the platinum electrode and the molten slag. The annular space between the inside of the insulating alumina tube and outside of the zirconia electrolyte tube was plugged with a sintered powder mixture of zirconia, alumina, and silica (1:1:0.01 by volume). The platinum electrode from the outside of the zirconia tube was insulated by another insulating tube and carried in the annular space between the zirconia and alumina tubes. This careful insulation was very important in order to detect the oxygen pressure change only at the bottom of the liquid slag. In the previous paper,[5] this insulation procedure seems not to have been successful. Thus, the measured EMF change for the previous study should be considered to be more or less a "mixed potential." Accordingly, the diffusion coefficient given in Fig. 8 in the previous paper was about twice that of the present results.

The reference electrode was composed of a platinum wire and a mixture of nickel and nickel oxide powder. A Pt-Pt, 13 pct Rh thermocouple was positioned beside

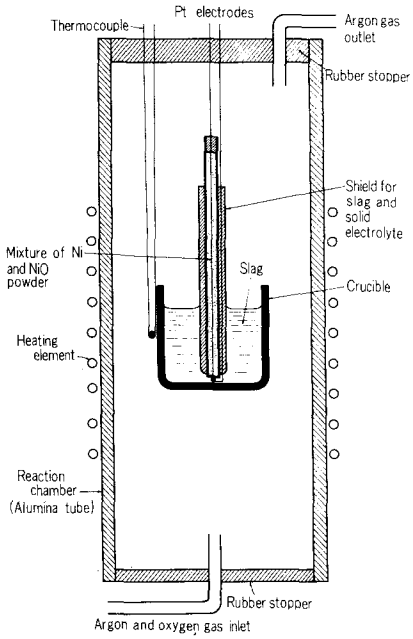

Fig. 3—Experimental apparatus for the measurement of oxygen diffusivity in molten slag.

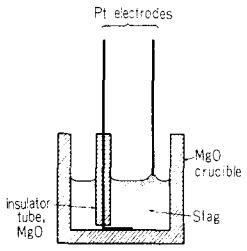

Fig. 4—Cell assembly with liquid slag as the electrolyte to detect the oxygen pressure change at the bottom of the slag (used only for the case of $CaO\text{-}SiO_2\text{-}Al_2O_3$ slags).

the outside wall of the fused alumina crucible. The crucible assembly was placed in the reaction chamber which was provided with a gas inlet and outlet. The dissolution of the alumina crucible in the liquid slag was insignificant during the experiments.

Fig. 4 shows the cell assembly which was used only for the experiments on liquid $CaO\text{-}SiO_2\text{-}Al_2O_3$ ternary slag. In this case, the slag itself functions as the electrolyte with the unit cation conductor.[20]

At the given temperature, the slag phase was equilibrated with a flow of air and thus oxygen gas was physically and/or chemically dissolved in the slag. Then, the air supply was very quickly stopped and argon gas with an oxygen pressure of 10^{-4} atm was supplied to the chamber. The dissolved oxygen then desorbed into the gas phase and the EMF (for example, initially about 600 mV at 1000°C) decreased as the oxygen diffused out.

The diffusion path could be little disturbed by the insertion of the oxygen concentration cell. Therefore, the diffusion problem was treated as a case of planar non-steady state diffusion neglecting the presence of the oxygen concentration cell. The magnitude of error due to this neglection is discussed later.

The oxygen content or oxygen pressure at the bottom of the slag column can be obtained from the solution of Fick's second law of diffusion. If one can assume that the oxygen content is proportional to the oxygen pressure, the EMF change, ΔE_t, during time, t, is as follows:

$$\Delta E_t = \frac{RT}{4F} \ln \frac{P_{O_2}^{\text{initial}}}{P_{O_2}^{t}} = \frac{RT}{4F} \ln \frac{[O_2]^i}{[O_2]^t}$$
$$= \frac{-RT}{4F} \ln \frac{4}{\pi} \sum_{n=0}^{\infty} \frac{(-1)^n}{(2n+1)} \exp\left\{\frac{-D(2n+1)^2\pi^2}{4L^2} t\right\} \qquad [7]$$

where R is the gas constant, T is the absolute temperature, F is the Faraday constant, $P_{O_2}^{\text{initial}}$ and $P_{O_2}^{t}$ are the oxygen pressures at the bottom of the melt before and after the change of the gas phase from air to argon, $[O_2]^i$ is the initial oxygen content and $[O_2]^t$ is the oxygen content at time, t, both at the bottom, L is the depth of slag, D is the diffusion constant of oxygen in the slag, and n is an integer starting from zero to infinity. This equation is valid only for large times, or for $D^2t \gg 4L^2$, and for example if t is larger than 500 s for $D = 10^{-4}$ cm^2/s, the error due to neglecting the second and other higher terms becomes less than 1 pct of D.

Neglecting the terms except the first term, Eq. [7] can be expressed by

$$\Delta E_t = -0.05212 \times 10^{-4} T + 0.5314 \times 10^{-4} \frac{DT}{L^2} t \qquad [8]$$

where ΔE_t is in volts, T is in K, L is in cm, D is in cm^2/s and t is in seconds. This derivation shows that the diffusion constant of oxygen can be obtained from the slope of the line of the EMF change against time, provided the solubility of the diffusing species is directly proportional to the oxygen partial pressure.

The absolute values of the oxygen partial pressure in the gas or liquid slag phases were determined using the standard free energy of formation of nickel oxide given by Coughlin,[27]

$$\Delta F_f^0 = -57{,}370 - 22.09T \text{ (K) (cal/mole NiO, 298 to 2000 K)} \qquad [9]$$

This equation was used in all cases, because the EMF of the cell for air or pure oxygen against a mixture of nickel and nickel oxide has been measured in a great number of experiments and it is very well confirmed that the EMF estimated from this equation agrees with the measured values within two millivolts at the present experimental temperature.

In order to determine the effect of the argon flow rate on the permeability, one experiment was made with the flow rate of 500 cc (STP)/min. The result, shown in Fig. 5, indicated no effect of the flow rate, and thus all other permeability experiments were made with a flow rate of 1500 cc (STP)/min.

II. EXPERIMENTAL RESULTS

Permeability

As an example, Fig. 5 shows how the EMF of the galvanic cell changed with time when various gases were supplied to the gas chambers, outside and inside of the shield tube (see Fig. 1). The initial oxygen pressure in the carrier gas was less than 10^{-8} atm, and was occasionally checked by the galvanic cell.

The part of the curve between A and B shows a gradual increase of oxygen pressure in the outlet-carrier gas when the atmosphere in the shield tube was changed from argon to pure oxygen. The EMF reached a constant value after about 80 min, indicating that the transport of oxygen gas through the liquid slag reached a steady state (from A to B in Fig. 5). When the EMF reached the steady state value, first air and then pure oxygen were introduced into the reaction chamber in order to calibrate the oxygen concentration cell (C is against air, and D is against oxygen in Fig. 5). The EMF values at C and D satisfied the calculated values. When argon was supplied again as the carrier gas, the EMF decreased with time and finally regained its initial constant value (the same EMF at B and E). Then the oxygen concentration cell was calibrated again using pure oxygen (F). Fig. 5 shows that the final steady state oxygen contents in the outlet gas were the same when approached from both higher and lower contents. The permeability was calculated from Eqs. [4] and [10]:

$$\mathbb{P} = K \cdot J \qquad [4]$$

$$J = \frac{1}{22.4 \times 10^3} \cdot V \cdot P_{O_2} \qquad [10]$$

where J is the rate of oxygen gas transfer through the liquid slag (moles O_2/s), V is the flow rate of carrier gas (STP cc/s), P_{O_2} is the oxygen partial pressure in the outlet-carrier gas at steady state. The cell constant K is defined by Eq. [2] (see Fig. 2).

Fig. 6 shows that the experimentally determined permeability is independent of the cell constant, satisfying Eq. [4] for a fixed composition and temperature.

Fig. 7 shows the relation between $-\log_{10} \mathbb{P}$ and $1/T$ for various compositions in the $PbO\text{-}SiO_2$ system with the range of the estimated relative errors. This figure shows that the permeability does not change very much with temperature. However, the permeability of oxygen gas in 100 pct PbO, 90 mol pct PbO-10 mol pct SiO_2 melts and 80 mol pct PbO-20 mol pct SiO_2 decreased slightly with temperature, while that in a 70 mol pct PbO-30 mol pct SiO_2 melt increased slightly with temperature. The permeability of oxygen gas in liquid $PbO\text{-}SiO_2$ melts decreased with an increase in SiO_2 content.

Diffusivity

As an example, Figs. 8 and 9 show the EMF change, ΔE_t, which is defined as the initial EMF minus the EMF at time t, for an 80 mol pct PbO-20 mol pct SiO_2 melt at various temperatures, and for a 40 wt pct CaO-40 wt pct SiO_2-20 wt pct Al_2O_3 melt at 1380°C, respectively. A linear relation was obtained between time and the EMF change except for the short initial period in accordance with Eq. [11]. In reality, ΔE_t was zero for

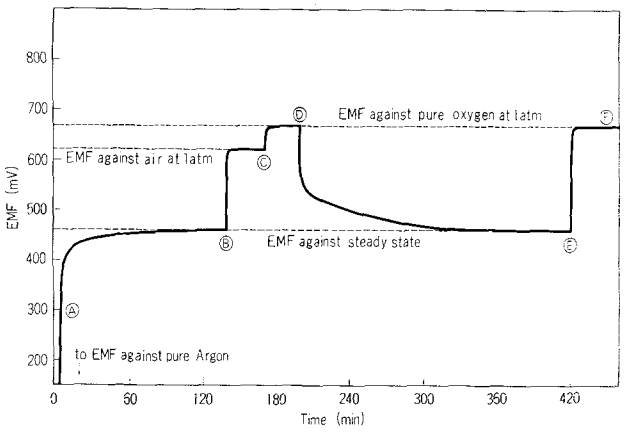

Fig. 5—EMF response to argon-oxygen mixtures in a permeability experiment, showing the calibration for air and pure oxygen (pure PbO at 1000°C, with an argon flow rate 500 cc (STP)/min).

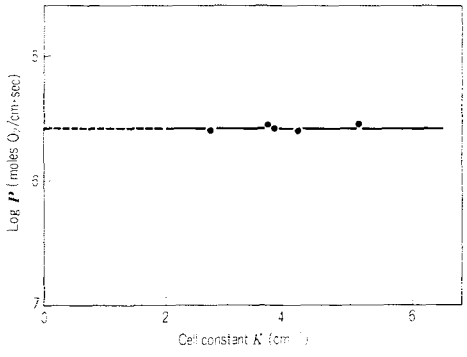

Fig. 6—Relation between the permeability of oxygen in liquid 2 mole pct FeO-88 mole pct $PbO\text{-}SiO_2$ at 1000°C and the cell constant, K.

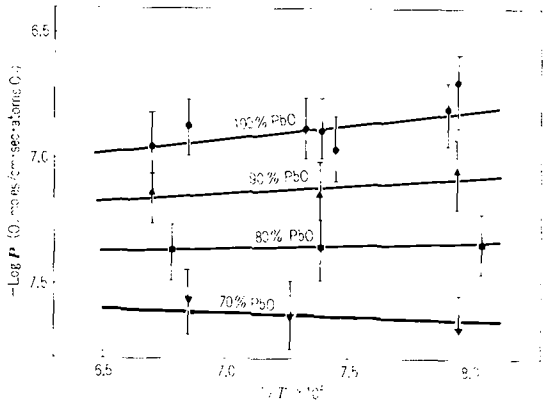

Fig. 7—Temperature dependency of oxygen permeability in the liquid PbO-SiO_2 system (in mole pct).

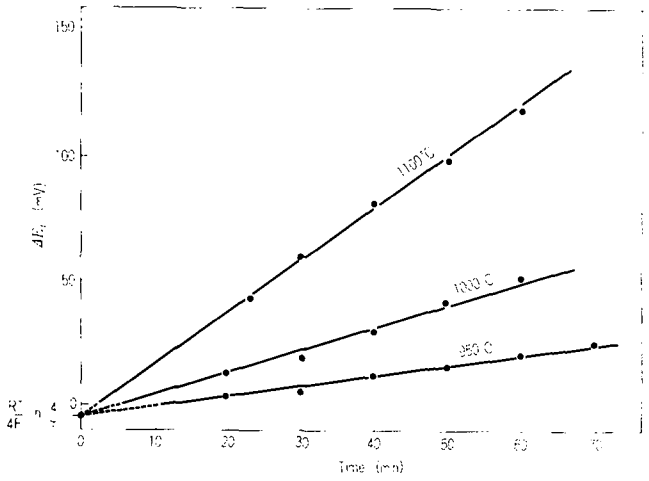

Fig. 8—Change of EMF with time in liquid 80 mol pct PbO-SiO_2.

this short initial period. Extrapolation of the lines to $t = 0$ intersect the ordinate at about $-(RT/4F)\ln(4/\pi)$. The crucible diameter and depth of the liquid was the same in the three runs for PbO-SiO_2 system.

If the rate of the EMF change is exclusively controlled by diffusion of oxygen gas in liquid slag, the diffusion coefficient can be calculated from Eq. [8]. However, Eq. [8] was slightly modified[21] to include the effect of the higher order terms in Eq. [7] as follows,[21]

$$\Delta E_t = 0.5115 \times 10^{-4}\,(D \cdot t \cdot T/L^2) - 0.05148 \times 10^{-4}\,T \qquad [11]$$

In our previous paper,[5] the dissolved oxygen in liquid oxide was assumed to be monatomic oxygen. However, because liquid oxide contains no free electrons as in a metal, diatomic oxygen with a predominate covalent bonding seems more likely to be the stable form. Thus, in the present paper, the apparent diffusion constant is assumed to be the diffusion constant of diatomic oxygen gas dissolved in the liquid oxide.

Figs. 10 and 11 show the relation between log D_{O_2} and $1/T$ for the various liquid oxide systems. In Fig. 11, the diffusion constants of helium in an oxide melt are plotted for comparison. Fig. 12 shows the relation between the apparent diffusion coefficient in FeO-PbO-SiO_2 and $1/T$. It is seen that the diffusion coefficient at lower temperatures is increased remarkably by the addition of a small quantity of iron oxide. This effect can be interpreted by the pronounced increase in oxygen transfer by the chemically-dissolved oxygen. However, this effect is not clearly seen at the higher temperatures.

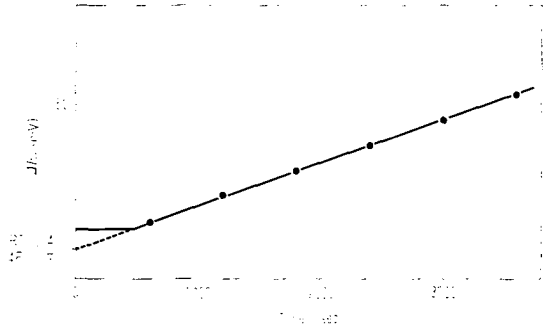

Fig. 9—Relation between EMF change, ΔE_t, and time in 40 wt pct CaO-40 wt pct SiO_2-20 wt pct Al_2O_3 at 1380°C.

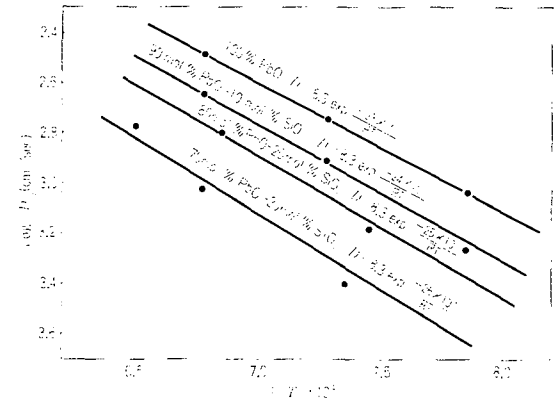

Fig. 10—Diffusion coefficient of oxygen gas in liquid PbO-SiO_2.

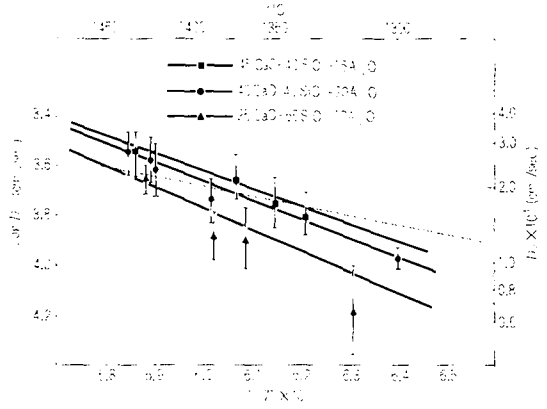

Fig. 11—Relation of $-\log D_{O_2}$ to $1/T$ for CaO-SiO_2-Al_2O_3 melts. The dotted line shows the He diffusion coefficient in 16 mol pct Na_2O-10 mol pct CaO-74 mol pct SiO_2.[6] (Simple pct means wt pct).

In Figs. 11 and 12, the range of the relative errors is given for each experimental run. The magnitude of the error is dependent mainly upon the melt depth, and is different for each run because of sometimes varying melt depths.

Because some of the results on the diffusion coefficients are not given in the figures, all the results are summarized in Table I.

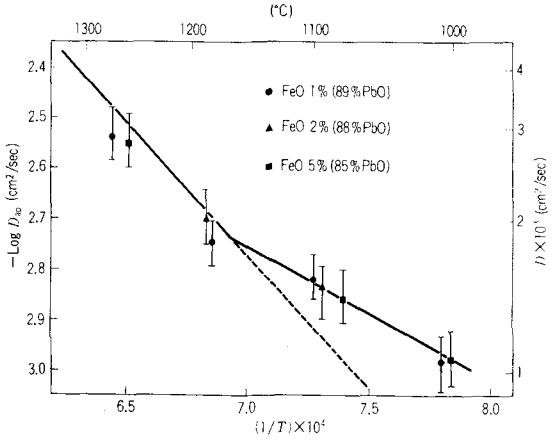

Fig. 12—Relation between apparent diffusion coefficient of oxygen and temperature in FeO-PbO-10 mol pct SiO_2. The dashed line shows the diffusion coefficient of oxygen gas in the 90 mol pct PbO-10 mol pct SiO_2 without FeO.

Table I. Summary of Experimental Results on the Permeability and Diffusivity of Oxygen

$\mathbb{P} = \mathbb{P}_0 \exp(-E/RT)$ (1000 to 1250°C)
$D = D_0 \exp(-E/RT)$ (1000 to 1450°C)

Slag Composition	$\mathbb{P}_0$(O_2 Mole/cm s)	E(kcal/mole O_2)
100 pct PbO	2.0×10^{-8}	−5.0
90 mol pct PbO-10 pct SiO_2	2.7×10^{-8}	−2.7
80 mol pct PbO-20 pct SiO_2	2.0×10^{-8}	−1.1
70 mol pct PbO-30 pct SiO_2	4.1×10^{-8}	+1.4
2 mol pct FeO-88 pct PbO-10 pct SiO_2	3.2×10^{-6}	10.0
Slag Composition	**D_0(cm²/s)**	**E(kcal/mol O_2)**
100 pct PbO	8.3	23
90 mol pct PbO-10 pct SiO_2	8.3	24
80 mol pct PbO-20 pct SiO_2	8.3	25
70 mol pct PbO-30 pct SiO_2	8.3	26
45 wt pct CaO-40 pct SiO_2-15 pct Al_2O_3	4.5	32.5
40 wt pct CaO-40 pct SiO_2-20 pct Al_2O_3	4.5	33.0
25 wt pct CaO-65 pct SiO_2-10 pct Al_2O_3	4.5	34.0
FeO-PbO-SiO_2		
Less than 5 mol pct FeO and lower than 1250°C	0.21	12.0
Less than 5 mol pct FeO and higher than 1250°C	same as PbO-SiO_2 without FeO	same as PbO-SiO_2 without FeO

III. DISCUSSION

Effects of Natural Convection on the Measured Permeability and Diffusivity

The maximum velocity of natural convection induced by a temperature difference for a fluid sandwiched by two parallel vertical plates is known to be proportional to the temperature difference of the two plates, the thermal expansion coefficient, and the reciprocal of the viscosity of the liquid,[22]

$$v_{max} = \frac{\bar{\rho}^2 \bar{\beta} 8 b^2 \Delta T}{32 \bar{\mu}} \qquad [12]$$

where v_{max} is the maximum velocity of natural convection in the vertical direction, $\bar{\rho}$ is the average density at mean temperature $\bar{T}$, $\bar{\beta}$ is the thermal expansion coefficient, b is one-half of the distance between the two plates, ΔT is the temperature difference, and $\bar{\mu}$ is the viscosity of the fluid. However, the present case would be with the convection between two horizontal planes.

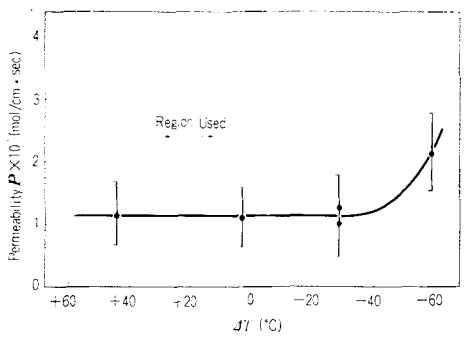

Fig. 13—Effect of temperature difference between top and bottom of the crucible on the measured permeability of oxygen gas in 100 pct PbO at 1000°C. (ΔT = temperature at slag surface − temperature at slag bottom).

Table II. Effect of Melt Size on the Diffusion Coefficient of Oxygen in Pure PbO at 1000°C

Depth of Slag (cm)	Diam of Crucibles (cm)	D_{O_2}(cm²/s)
0.93	1.2	9.6×10^{-4}
2.41	1.2	10.0×10^{-4}
1.00	3.5	9.8×10^{-4}

A well-established equation as the above is not available for this case but the magnitude of convection seems proportional to β/μ from this equation.[22] Therefore, one may assume a similar type of function for convection in slag in the present experiments, where the shape of the cell assembly is fixed and the temperature is different between the top and the bottom of the crucible. Thus, if convection is experimentally known to be negligible for pure PbO with $\beta\bar{\rho}^2/\bar{\mu}$ equal to about 4.3×10^{-3} ($g \cdot s^{-1} \cdot cm^{-5} \cdot deg^{-1}$), then natural convection in the other cases with smaller values ($\beta\bar{\rho}^2/\bar{\mu}$ for PbO-10 mol pct SiO_2 and PbO-30 mol pct SiO_2 at 1000°C is 2.2×10^{-3} and 1.5×10^{-3}, respectively) can be neglected. Natural convection in the liquid slag can be prevented if the temperature at the top of the crucible is controlled to be higher than at the bottom, *i.e.*, with a higher density at the bottom. Fig. 13 shows the relation of the temperature difference between the top and bottom of the crucible to the measured permeability of oxygen in pure PbO at 1000°C (the inner diameter of the crucible was 20 mm and the depth of slag was 20 mm). It is seen that natural convection does not affect the measured permeability, as long as the temperature at the top is higher than at the bottom. Thus, in the all experiments, the temperature at the top of the crucible was controlled to be about 20°C higher than at the bottom.

Furthermore, different crucible diameters and slag depths were used in the diffusivity measurements to check the effect of these dimensions upon the diffusivity obtained. Table II shows the results for pure PbO; in spite of the difference in the dimensions of the melts, the diffusion coefficients were nearly same. From the above experiments, it seemed that the error due to natural convection was much less than to other sources of experimental error.

Estimation of the Relative Experimental Error

The relative error in the permeability can be determined from Eq. [4] as follows:

$$d\mathbb{P}/\mathbb{P} = dK/K + dV/V + dP_{O_2}/P_{O_2} \quad [13]$$

Differentiation of

$$E = \frac{RT}{4F} \ln \frac{P_{O_2}}{P^0_{O_2}} \quad (P^0_{O_2} \text{ is a constant value}) \quad [14]$$

gives

$$dE/E = dT/T + d \ln P_{O_2}/\ln P_{O_2} = dT/T + (dP_{O_2}/P_{O_2}) \ln P_{O_2} \quad [15]$$

From Eqs. [13] and [15], one then has the following expression

$$d\mathbb{P}/\mathbb{P} = dK/K + dV/V + \ln P_{O_2} (dE/E - dT/T) \quad [16]$$

The relative errors in each of the experimentally measured quantities are approximately estimated as follows,

$dK/K = \pm 20$ pct, $dV/V = \pm 10$ pct, $dE/E = \pm 0.01$ pct,

$dT/T = \pm 1$ pct,

and P_{O_2} is about 10^{-5}. Then the relative error in the permeability can be estimated from

$$d\mathbb{P}/\mathbb{P} = \pm 20 \text{ pct } \pm 10 \text{ pct} - 5 \times 2.3 \times (\pm 0.01 \pm 1) \text{ pct} = \pm 40 \text{ pct (as shown in Fig. 7).}$$

Similarly, the error in the diffusivity is calculated as follows:

$$dD/D = dE/E + dt/t + dT/T + 2dl/l \quad [17]$$

The individual errors are estimated to be approximately as follows;

$dE/E = \pm 0.01$ pct, $dt/t = \pm 0$ pct and $dT/T = \pm 1$ pct.

The value for dl/l was estimated to be -5 pct and $+10$ pct, because the true diffusion path is always longer than the melt depth due to the insertion of the oxygen cell (see Fig. 3). Thus, the total error becomes -11 pct and $+21$ pct.

Transport Mechanism of Oxygen

Two transport mechanisms are conceivable for the diffusion of oxygen in PbO-SiO_2 melts unter our experimental conditions: the diffusion of physically dissolved oxygen gas as expressed by Eq. [1], and the diffusion of chemically dissolved oxygen gas (oxygen anions) as expressed by Eq. [2]. The latter mechanism is well known as Wagner's theory[23] which has been proved by experiments on transition metal solid oxides at elevated temperatures.

If oxygen transfer in the present experiments was exclusively by the diffusion of chemically-dissolved oxygen (divalent oxygen anions), then Wagner's theory should be satisfied by the present results. According to Wagner's theory, the rate of transfer through the liquid oxide can be expressed for the present experimental conditions as follows;

$$\mathbb{P} = KJ_{O_2} = \frac{RT}{16F^2F'} \int_{P_{O_2(I)}}^{P_{O_2(II)}} \sigma t_e d \ln P_{O_2} \quad [18]$$

where J_{O_2} is the oxygen transfer rate (moles O_2/s), R is the gas constant (1.98 cal/mol deg), T is the temperature (K), both F and F' are the Faraday constant (F = 23070 cal/mol volt eq. and F' = 96500 A-s/eq.), K is the cell constant defined by Eq. [4] (cm^{-1}), σ is the specific conductivity (A/volt.cm), t_e is the transference number of electrons, P_{O_2}(I) is the oxygen partial pressure in the carrier gas and P_{O_2}(II) is the oxygen pressure of pure oxygen in the shield pipe (see Fig. 1).

For example at 1100°C, the oxygen transfer rate can be estimated from the above equation. The conductivity[24] of a pure PbO melt, σ, is about 2.0 A/volt.cm and of a 70 mol pct PbO-30 mol pct SiO_2 melt it is about 0.9 A/volt.cm. Ito and Yanagase[25] reported that the ionic transference number of these two melts is essentially unity. However, estimating the magnitude of their experimental errors, it seems that the maximum transference number of electrons could be assumed to be the order of 10^{-3}. Therefore, the permeability, $\mathbb{P}_{cal}$, can be calculated from Eq. [18]. In the cases of pure PbO and 70 pct PbO-30 pct SiO_2, the oxygen pressures in the outlet gas (P_{O_2}(I)) are 5.5×10^{-5} atm and 9.1×10^{-6} atm, respectively.

$$\mathbb{P}_{cal}(PbO, 1100°C) = \frac{1.98 \times 1373}{16 \times 23070 \times 96500} (2.0 \times 1 \times 10^{-3}) \cdot \{\ln 1 - \ln 5.5 \times 10^{-5}\} = 7.5 \times 10^{-9} \ (O_2 \text{ moles/s.cm})$$

Similarly, for 70 mol pct PbO-30 mol pct SiO_2, the permeability can be estimated to be 0.8×10^{-9} (O_2 moles/s.cm).

These permeabilities are smaller than those measured by a factor of one hundred for pure PbO and fifty for the PbO-SiO_2 melt. (This is true only for PbO-SiO_2 melts.)

Therefore, diffusion of chemically dissolved oxygen gas (O^{2-}) can be judged to play a minor part in the oxygen transfer mechanism under the present experimental conditions. The major mechanism, which is supported by the present results, seems to be the diffusion of physically dissolved oxygen.

Estimation of Physical Solubility of Oxygen Gas in PbO-SiO_2 Melts

Because the permeability and the diffusivity are independently measured, the physical solubility of oxygen gas in PbO-SiO_2 melts can be estimated from Eq. [19].

$$\mathbb{P} = D_{O_2} (C^0_{O_2} - C_{argon}) \quad [19]$$

where $\mathbb{P}$ is the permeability, D_{O_2} is the diffusivity of oxygen gas in liquid slag, $C^0_{O_2}$ is the oxygen concentration in liquid slag equilibrated at 1 atm oxygen gas, and C_{argon} is the oxygen concentration in liquid slag equilibrated with argon gas. C_{argon} could be taken to be zero, because P_{O_2} in the argon carrier gas was in the range of 10^{-4} to 10^{-6} atm. Fig. 14 shows the estimated solubility of oxygen gas in the liquid PbO-SiO_2 system under 1 atm oxygen gas. The mean values of diffusivity and permeability at each temperature are used in the calculations. From this figure, the dissolution of oxygen into the melts seems to be an exothermic reaction with a heat of dissolution of about -29 kcal/mole O_2.

The physical solubility of gaseous elements (helium etc) and metals (Au etc) have been studied by a few workers.[6,8,10,11] Mulfinger and Scholze[6] measured the solubility of helium gas in Na_2O-CaO-SiO_2, Na_2O-CaO-Al_2O_3, K_2O-SiO_2, Na_2O-SiO_2 and Li_2O-SiO_2 melts at 1200 to 1480°C. Their results indicated that the solu-

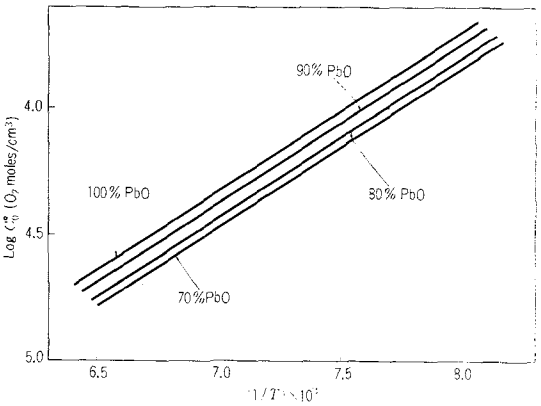

Fig. 14—Estimated solubility of oxygen gas in liquid $PbO-SiO_2$ under 1 atm oxygen gas.

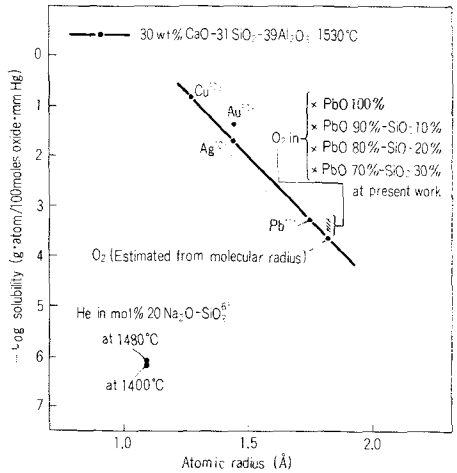

Fig. 15—Relation between logarithm of solubility of neutral atoms or molecules in liquid slag and atomic or molecular diameter. (Solid line is reproduced from Ref. 11).

bility increased with temperature and with the content of network-forming oxides, *e.g.*, SiO_2 or Al_2O_3. Thus, they concluded that the helium atoms are accommodated in electrically-neutral holes of the liquid structure of the oxide melts, the concentration of which seems to increase with temperature and the content of acidic oxides. Richardson and his coworkers[10,11] determined the physical solubility of the neutral metals Au, Ag, Pb, and Cu in $CaO-SiO_2-Al_2O_3$ melts. The solubility increased with temperature and the silica content, similarly to the case for helium. At a fixed temperature of 1530°C, a vapor pressure of metal of 1.0 mm Hg, and a fixed slag composition, the physical solubility decreased with increasing atomic radius as shown in Fig. 15. In this figure, the results of Mulfinger and Scholze[6] and those of the present study are converted to the solubility under a 1 mm Hg vapor pressure and plotted for comparison. Here, the molecular radius of O_2 gas at 25°C (1.82Å) was used for the plot. From this figure, it seems that the physical solubility depends very much on the slag composition but not much on the temperature.

Contrary to other studies,[6,10,11] the present results indicated that the solubility decreases with an increase in silica content in the range of 100 pct to 80 pct PbO, and increases slightly between 80 pct and 70 pct PbO. However, in the range of pure PbO down to 70 mol pct PbO, the molar volume of the melt decreases with increasing silica content.[26] Thus, it can be assumed, in agreement with the present results, that the concentration of neutral holes decreased with silica content in this composition range. Other workers[6,10,11] used a more acidic composition than in the present study, where the molar volume seems to increase with increasing silica content (the necessary density to estimate the exact molar volumes are not available).

In the present study, the oxygen solubility in basic melts decreased with temperature, while it increased with temperature in the more acidic melts in previous studies.[6,10,11] Thus, it can be deduced that the "effective" volume or "effective" content of holes in the very basic melts decreases with temperature because of the thermal vibration of cations and free oxygen anions, although the molar volume increases with temperature. These considerations suggest that the relation between the solubility and temperature or the content of network formers would change for extremely basic or acidic compositions.

The product of the solubility and diffusivity of oxygen in barium-alumina-alkali-silicate melts can be estimated to be in the range of 10^{-12} to 10^{-10} moles/cm·s at 1000 to 1300°C from the slope of the curves in Figs. 5 and 6 of the paper by Greene and Gaffney.[1]

Although the experimental errors are not always small in this kind of high temperature experiment, this large difference between the values suggests that the product of the solubility and diffusivity does depend very much upon the composition of oxide melts. (Compare Figs. 10 and 11 for a relatively large difference in the diffusivities in $PbO-SiO_2$ melts and $CaO-SiO_2-Al_2O_3$ melts.)

IV. CONCLUSION

An experimental procedure for the measurement of the permeability of dissolved oxygen in liquid slag has been developed using an oxygen concentration cell. The small amount of oxygen gas which permeated through the liquid oxide from the pure oxygen compartment to the pure argon compartment was determined by the galvanic cell. The permeabilities of oxygen through liquid $PbO-SiO_2$ and $FeO-PbO-SiO_2$ at 1000 to 1250°C were in the range of 3×10^{-8} to 3×10^{-7} moles/cm·s. The permeability was little influenced by temperature but more influenced by composition.

Independently from the above method, an experimental procedure for the determination of the diffusion coefficient of dissolved oxygen in liquid slag has been developed using an oxygen concentration cell. In this method it is not necessary to quench the specimen to determine the concentration profile of dissolved oxygen. Instead, the oxygen pressure change at the bottom of the slag column was detected by the galvanic cell.

Liquid oxides in the $PbO-GeO_2$, Na_2O-GeO_2, $CaO-SiO_2-Al_2O_3$ and $FeO-PbO-SiO_2$ systems were studied. The diffusion coefficients determined are in the range of 5×10^{-5} to 3×10^{-3} cm^2/s at 1000 to 1450°C. The diffusion coefficients increase with temperature for fixed compositions of slag. The coefficients increase with an increase in the content of network-modifying oxides at constant temperature.

The solubility of oxygen gas in $PbO-SiO_2$ melts was estimated to be 2×10^{-4} to 2×10^{-5} moles/cm^3 from the

determined diffusivity and permeability. The solubility decreased slightly with an increase in silica content in the present composition range and with an increase in temperature.

Physical solubilities of gases and metals in molten slags determined by other investigators are compared to the present results.

ACKNOWLEDGMENTS

The authors would like to express sincere gratitude to Dr. S. G. Whiteway, National Research Council of Canada, Halifax, Nova Scotia, for his numerous constructive comments on this manuscript.

REFERENCES

1. C. H. Greene and R. F. Gaffney: *J. Amer. Ceram. Soc.*, 1959, vol. 42, pp. 271-75.
2. C. H. Greene and I. Kitano: *Glastech. Ber.*, 1959, vol. 32K, pp. V44-48.
3. C. Wagner: Max-Planck-Inst. für Phys. Chem., Göttingen, private communication to K. S. Goto, at Max-Pl-Inst. für Metallforschung, Stuttgart, May, 1970.
4. K. S. Goto, M. Sasabe, and M. Someno: *Trans. TMS-AIME*, 1968, vol. 242, pp. 1757-59.
5. M. Sasabe, K. S. Goto, and M. Someno: *Met. Trans.*, 1970, vol. 1, pp. 811-17.
6. H.-O. Mulfinger and H. Scholze: *Glastech. Ber.*, 1962, vol. 35, pp. 466-78 and 495-500.
7. G. H. Frischat and H. J. Oel: *Phys. Chem. Glasses*, 1967, vol. 8, pp. 92-95.
8. H.-O. Mulfinger and H. Meyer: *Glastech. Ber.*, 1963, vol. 36, pp. 481-83.
9. H.-O. Mulfinger: *J. Amer. Cer. Soc.*, 1966, vol. 49, pp. 462-66.
10. F. D. Richardson and J. C. Billington: *Trans. Inst. Mining Metall.*, 1955, vol. 56, pp. 273-97.
11. H. W. Meyer and F. D. Richardson: *Trans. Inst. Mining Metall.*, 1961-62, vol. 71, pp. 201-14.
12. E. A. Mizukar, R. E. Grace, and N. A. D. Parlee: *Trans. Amer. Soc. Metals*, 1963, vol. 56, p. 101.
13. H. Rickert and A. A. ElMiligy: *Z. Metallk.*, 1968, vol. 59, p. 635.
14. N. A. D. Parlee and H. Seibel: *Trans. TMS-AIME*, 1965, vol. 233, p. 1923.
15. L. R. Velho, N. M. El-Tayeb, J. Gani, and N. A. D. Parlee: *Trans. TMS-AIME*, 1969, vol. 254, p. 184.
16. C. R. Masson and S. G. Whiteway: *Can. Met. Quarter.*, 1967, vol. 6, pp. 199-217.
17. N. Sano, S. Honma, and Y. Matsushita: *Trans. J. Iron Steel Inst.*, 1969, vol. 9, pp. 404-08.
18. A. Siebelts and J. Hagenacker: *Z. Phys. Chem.*, 1909, vol. 68, pp. 10115-28.
19. C. J. Smithells: *Metals Reference Book*, 3rd ed., Vol. II, Butterworths, 1962.
20. K. Sanbongi and Y. Oomori: *Nippon Kinzoku Gakkaischi (J. Jap. Inst. Metals)*, 1957, vol. 21, pp. 296-300.
21. This eq. was obtained from Fig. 4-1 in page 46 of *The Mathematics of Diffusion*, by J. Crank, Oxford Press, 1964.
22. R. B. Bird, W. E. Stewart, and E. N. Lightfoot: *Transport Phenomena*, John & Wiley, 1960, pp. 297-300.
23. C. Wagner: *Z. Phys. Chem.*, 1933, Vol. B21, pp. 25-41.
24. H. Saito, K. Goto, and M. Someno: *Tetsu-to-Hagane*, 1969, vol. 55, pp. 539-49.
25. H. Ito and T. Yanagase: *Denki-Kagaku*, 1958, vol. 26, pp. 363-65.
26. H. Ito and T. Yanagase: *Trans. J. Inst. Metals*, 1960, vol. 1, pp. 116-20.
27. J. P. Coughlin: U.S. Bureau of Mines Bull., No. 542, 1954.